

## Energy-resolved photofield emission from the W(100) surface state

Y. Gao and R. Reifenberger

*Department of Physics, Purdue University, West Lafayette, Indiana 47907*

(Received 7 December 1984; revised manuscript received 11 March 1985)

Measurements of the photofield current emitted at energies below threshold ( $\hbar\omega < \Phi$ ) from the W(100) surface state clearly show initial-state structure in the final-state energy distributions obtained at these low photon energies. Analysis of data taken as a function of the polarization vector of the incident light shows that photoemission from the surface state is not strongly influenced by the coupling between components in the vector potential induced by the spatial variation of  $\mathbf{A}$  near a metal surface.

A new technique has been under development that can address the nature of the photoexcitation process at low photon energies not normally accessible using standard photoemission procedures.<sup>1-4</sup> This experimental technique is characterized by incident photon energies  $\hbar\omega$  which are less than the work function  $\Phi$  of the emitting surface. The photoexcited electrons escape into the vacuum at energies below threshold by applying a sufficiently strong electric field ( $\sim 10^9$  V/m) to the surface of the emitting material. The electric field distorts the surface potential barrier, normally assumed to be a square step, into a triangular shape characterized by a finite width. This permits electrons photoexcited into final states below threshold to quantum mechanically tunnel into the vacuum. Because of this tunneling mechanism, the technique is ideally suited for investigation of photoexcited energy distributions at low photon energies since the escape conditions normally invoked when  $\hbar\omega \sim \Phi$  are no longer applicable. All previous studies of the final states probed by this photofield emission technique have yielded smooth, triangular-shaped distributions in which joint density-of-state effects expected from bulk band-structure calculations have been absent.<sup>1-7</sup>

We report new measurements performed to study the polarization dependence of the photocurrent at these low photon energies from W(100). In contrast with previous work, these new measurements employ a dispersive 127° velocity selector energy analyzer. This results in an improved signal-to-noise ratio and reveals structure in the final-state photodistributions. W(100) is known to have a surface state located  $\sim 0.35$  eV below  $E_F$ . The existence of this state was first observed in field emission experiments<sup>8</sup> and has been studied experimentally using photoemission techniques<sup>9</sup> at high ( $\hbar\omega > 20$  eV) photon energies. Calculations have estimated that as much as 90% of this state is located within the first atomic layer of the W(100) surface.<sup>10</sup> It therefore serves as an excellent initial-state "marker" to use in studies of subthreshold photoemission.

Figure 1 shows the energy distribution spectrum obtained from W(100) subjected to an electric field  $F = 2.8 \times 10^9$  V/m and illuminated with laser light of energy  $\hbar\omega = 2.61$  eV. The experimental apparatus has been described elsewhere.<sup>7,11</sup> Briefly, it consists of a 127° energy analyzer with an energy resolution better than 0.07 eV. The entire apparatus is enclosed in a UHV stainless steel chamber that operates in the mid- $10^{-11}$ -Torr regime. The emitting surface is the end form of a thin wire etched to submicron dimensions. Two separate distributions are evident in Fig. 1. One is due to electrons field emitted from W(100) at energies near  $E_F$ .

The enhanced emission observed at energies  $\sim 0.35$  eV below  $E_F$  is due to the W(100) surface state. The other distribution, centered at  $E - E_F \sim 2.6$  eV, is due to photoexcited electrons. The improved signal-to-noise ratio of the 127° energy analyzer clearly reveals that a large contribution from the surface state is present. These data provide the first convincing evidence for initial-state structure in subthreshold photoemission experiments.

Since the initial states contributing to the structure in the photoexcited distribution are localized within the first atomic layer, it is of interest to investigate how the photoexcitation probability depends on the polarization vector of the incident light. This analysis is facilitated by using a theory of photofield emission recently devised by Schwartz and Cole that is based on a free-electron model.<sup>12</sup> In their theory, the total energy distribution of photofield emitted electrons,  $j_p'(E)$ , at fixed electric field  $F$  as a function of the final-state energy  $E$  is written as the product of the Fermi-Dirac distribution function  $f(E - \hbar\omega)$  shifted upward by the photon energy, the supply function  $N_p$ , a transmission probability  $D(E_z)$ , where  $E_z = E - \hbar^2 k_{\parallel}^2 / 2m$ , and a transition probability  $M_{if}$  between initial and final states:

$$j_p'(E) \propto f(E - \hbar\omega) \int_{E_z} N_p(E_z, E) D(E_z) |M_{if}|^2 dE_z \quad (1)$$

In implementing this model we have numerically evaluated

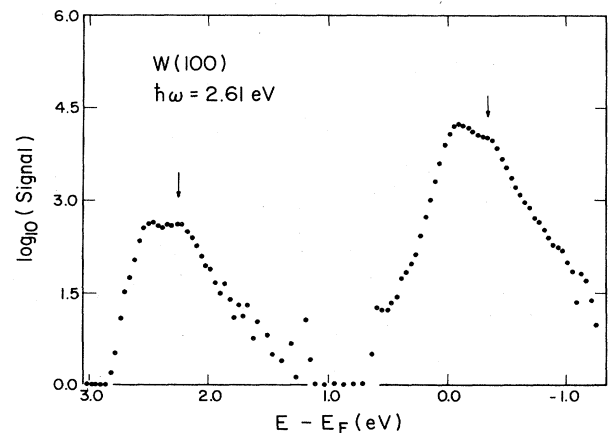


FIG. 1. Plot of the logarithm of the detected signal vs the final-state energy of electrons emitted from W(100). The data were obtained by illuminating a tungsten field emission tip by the focused beam of an argon-ion laser tuned to the 2.61-eV line.

the transmission probabilities  $D(E_z)$  through an image rounded surface potential barrier.<sup>13</sup> In what follows, the magnitude of the transition probability  $M_{if}$  has been set to a constant and only the polarization dependence of  $M_{if}$  is emphasized.

Typical fits to the photodistributions from W(100) for three different polarizations of the incident light are shown in Fig. 2. The relevant geometrical considerations are shown in the inset of this figure. By subtracting the expected signal [given by Eq. (1)] from the experimental distributions, the strength of the surface-state feature can readily be determined as illustrated by the solid squares in Fig. 2.

The polarization dependence of the subthreshold photo-

signal can be analyzed through the matrix element  $M_{if}$ :

$$M_{if} = \langle f | \mathbf{A} \cdot \mathbf{p} + \mathbf{p} \cdot \mathbf{A} | i \rangle, \quad (2)$$

where  $\mathbf{A}$  is the vector potential of the incident light,  $\mathbf{p}$  the momentum operator, and  $\langle f |$  and  $| i \rangle$  are the final- and initial-state wave functions, respectively. This can be rewritten as<sup>14</sup>

$$M_{if} = \frac{-i}{\hbar\omega} (\langle f | \mathbf{A} \cdot \nabla V_B | i \rangle + \langle f | \mathbf{A} \cdot \nabla V_S | i \rangle) - i \langle f | \left. \frac{\partial \mathbf{A}}{\partial z} \right| i \rangle, \quad (3)$$

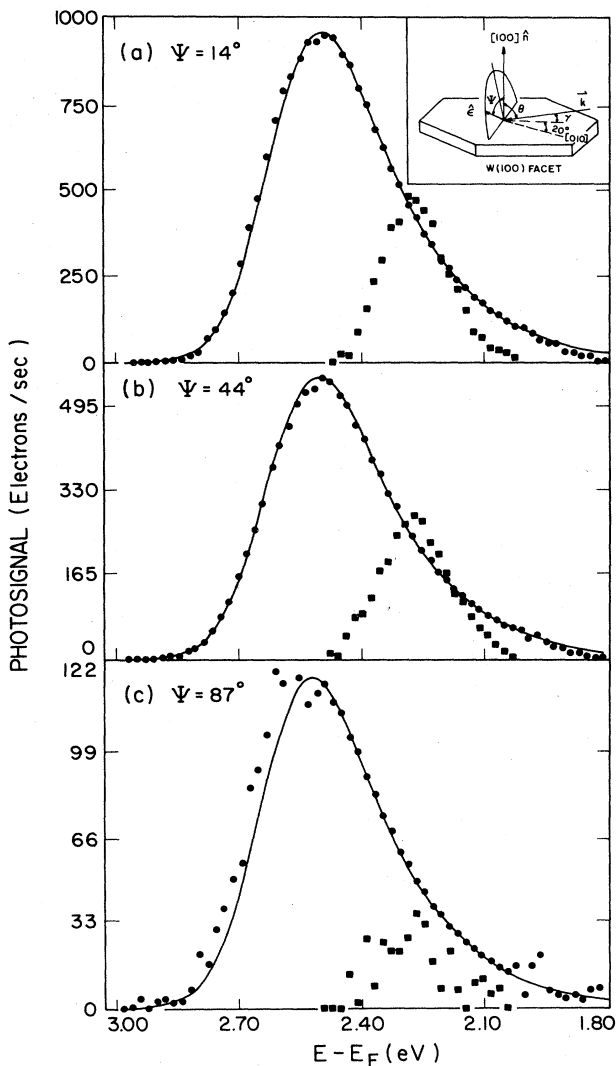


FIG. 2. Plots of the polarization dependence of the photosignal from W(100). The inset shows the relevant geometrical considerations. The angle of incidence of the input light is  $\pi/2 - \gamma = 76^\circ$ . The photosignal has been separated into the expected photofield contribution [solid dots, experiment; solid line, theory from Eq. (1)] and the emission from the W(100) surface state (solid squares). (a), (b), and (c) are for polarization vectors making an angle of  $14^\circ$ ,  $44^\circ$ , and  $87^\circ$  with respect to the W(100) surface normal  $\hat{n}$ . When  $\Psi = 90^\circ$ , the incident light is  $s$  polarized.

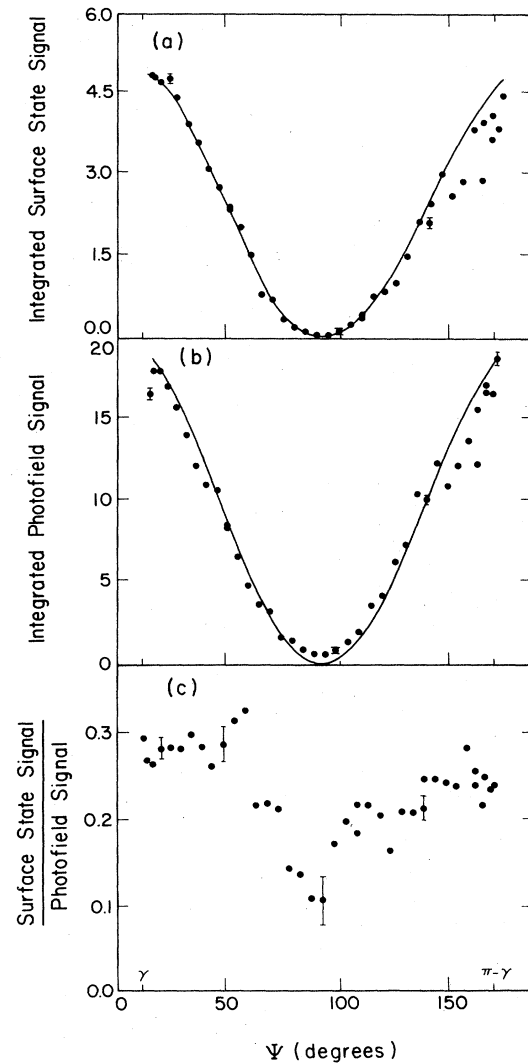


FIG. 3. Polarization dependence of the photosignal from W(100). (a) shows the polarization dependence of the surface state emission as a function of the angle  $\Psi$  between the polarization vector  $\hat{\epsilon}$  and the W(100) surface normal  $\hat{n}$ . (b) is a similar plot of the experimental photofield signal expected on the basis of Eq. (1). The solid lines in (a) and (b) show  $2 \cos^2 \Psi$  behavior. (c) illustrates the ratio of these two components in the subthreshold photosignal as a function of the angle  $\Psi$ . The sharp decrease in this ratio when  $\Psi = 90^\circ$  ( $s$  polarization) indicates that different excitation mechanisms are responsible for the photoexcitation of the surface state and the photofield emission feature.

where  $\nabla V_B$  and  $\nabla V_S$  are the gradients of the bulk and surface potential influencing the excited electron state. Expanding the potential in the bulk by a Fourier series over all reciprocal lattice vectors  $\mathbf{G}$ , the first term in Eq. (3) acquires a well known polarization dependence given by  $\hat{\epsilon} \cdot \mathbf{G}$  with  $\hat{\epsilon}$  a unit vector directed along  $\mathbf{A}$ . The second term in Eq. (3) is dominated by the  $z$  component of the surface potential, which in these experiments can be approximated by a step-function discontinuity in the potential barrier located at the metal-vacuum interface. This term results in a polarization dependence given by  $\hat{\epsilon} \cdot \hat{n}$  where  $\hat{n}$  is a vector directed normal to  $W(100)$ . The third term in Eq. (3) is due to the surface field effect which describes the strong spatial variation of the electromagnetic wave as it enters a metal surface. Theoretical work on various model systems has shown that such variations can be estimated by a proper accounting of nonlocal screening effects that occur at a metal-vacuum interface.<sup>15,16</sup> The polarization dependence of this term depends on how strongly longitudinal components in  $\mathbf{A}$  are produced within a few angstroms of the metal surface. If the conductivity tensor at a metal-vacuum interface is significantly different from its bulk jellium value, the polarization dependence ascribed to this third term will be quite complicated and different than the simple polarization dependence appropriate for the first two terms in Eq. (3). Otherwise, the surface field effect will have a similar polarization dependence as the second term in Eq. (3).

It is reasonable to assume that photoemission from the  $W(100)$  surface state is entirely governed by the second and third terms in Eq. (3) since  $\nabla V_S$  and  $\partial \mathbf{A} / \partial z$  are both expected to be large at the metal-vacuum interface. Thus, by measuring the observed surface state photosignal versus the polarization of the incident light, the relative importance of these two terms may be assessed. The results of such an analysis are shown in Fig. 3(a), which plots the integrated surface-state photosignal as a function of polarization for the incident light. The small but nonzero signal observed even when  $\Psi = \pi/2$  is attributed to diffraction effects of the light in the vicinity of the field emission tip. The observed polarization dependence is consistent with the  $d_2$  character of this surface state. Also plotted as a solid line is the expected  $\cos^2\Psi$  behavior based on the assumption that the second term in Eq. (3) is dominant or that the coupling between the components in the vector potential by the spatial variation of  $\mathbf{A}$  is small. The agreement between theory,

based on a bulk jellium model which shows a weak coupling between the various components of  $\mathbf{A}$ , and experiment is quite reasonable.

Also shown in Fig. 3(b) is the polarization dependence of the integrated photofield energy distribution. The solid line again shows a  $\cos^2\Psi$  polarization dependence. In contrast with the behavior found for emission from the surface state, the photofield emission feature does not decrease as rapidly as a function of the polarization of the incident light. We find it useful to plot the ratio of the photocurrent emitted from the surface state to the current emitted from the photofield energy distribution as a function of polarization. If identical terms in Eq. (3) are responsible for the photoexcitation of both the surface state and the photofield emission feature, this ratio should yield a constant independent of the orientation of the polarization vector with respect to the emitting surface. Such a plot is given in Fig. 3(c) and clearly shows that the polarization dependence of photoexcitation from the surface state is different than that governing the photofield emission feature.

Possible contributions to the photofield current from  $\mathbf{G}_{100}$  in the first term in Eq. (3) can be ruled out by noting that the expansion of  $V_B$  does not contain a contribution from  $\mathbf{G}_{100}$  since this Fourier component vanishes for a bcc lattice due to structure factor considerations. This eliminates the possibility that the observed polarization dependence in this photoemission feature arises from a bulk photoexcitation process supported by  $\mathbf{G}_{100}$ .<sup>17</sup> Emission from the bulk at oblique angles is possible but should be small because of the strong selection of normal emission favored by transmission through the image-rounded surface potential barrier. We conclude that the origin of this nonzero photofield current for  $s$ -polarized light can be attributed to this oblique bulk emission effect.

This work was supported by U.S. Department of Energy Contract No. DE45162. The use of the National Science Foundation Materials Research Center (NSF/MRL) Central Laser Facility at Purdue supported in part by NSF/MRL Grant No. 80-22868 is also acknowledged. One of us (Y.G.) would like to thank the David Ross Foundation for financial support. We would like to thank M. J. G. Lee for informing us that initial-state effects in photofield emission have also been recently observed from  $W(111)$ . The initial assistance of Dr. C. M. Egert and Dr. D. L. Haavig with the design of the experimental apparatus is gratefully appreciated.

<sup>1</sup>M. J. G. Lee, Phys. Rev. Lett. **30**, 1193 (1973).

<sup>2</sup>T. Radon and Ch. Kleint, Surf. Sci. **60**, 540 (1976).

<sup>3</sup>Y. Teisseyre, R. Haug, and R. Coelho, Surf. Sci. **87**, 549 (1979).

<sup>4</sup>R. Reifenger, C. M. Egert, and D. L. Haavig, J. Vac. Sci. Technol. A **2**, 927 (1984); C. M. Egert and R. Reifenger, Surf. Sci. **145**, 159 (1984).

<sup>5</sup>R. Reifenger, H. A. Goldberg, and M. J. G. Lee, Surf. Sci. **83**, 599 (1979).

<sup>6</sup>D. Venus and M. J. G. Lee, Phys. Rev. B **28**, 437 (1983).

<sup>7</sup>D. L. Haavig and R. Reifenger, Surf. Sci. **151**, 128 (1985).

<sup>8</sup>L. W. Swanson and L. C. Crouser, Phys. Rev. **163**, 622 (1967).

<sup>9</sup>S.-L. Weng, E. W. Plummer, and T. Gustafsson, Phys. Rev. B **18**, 1718 (1978).

<sup>10</sup>M. Posternak, H. Krakauer, A. J. Freeman, and D. D. Koelling,

Phys. Rev. B **21**, 5601 (1980).

<sup>11</sup>Y. Gao, R. Reifenger, and R. Kremer, J. Phys. E **18**, 381 (1985).

<sup>12</sup>C. Schwartz and M. W. Cole, Surf. Sci. **115**, 290 (1982).

<sup>13</sup>R. Reifenger, D. L. Haavig, and C. M. Egert, Surf. Sci. **109**, 276 (1981).

<sup>14</sup>B. Feuerbacher and R. F. Willis, J. Phys. C **9**, 169 (1976).

<sup>15</sup>K. L. Kliewer, in *Photoemission and Electronic Properties of Surfaces*, edited by B. Feuerbacher, B. Fitton, and R. F. Willis (Wiley, New York, 1978), p. 45; Phys. Rev. B **14**, 1412 (1976).

<sup>16</sup>P. J. Feibelman, Phys. Rev. B **12**, 1319 (1975).

<sup>17</sup>Bulk photoemission may also be supported by  $\mathbf{G}_{200}$  but this contribution is of higher order and expected to be quite small.